CHAPTER V
ITRAQ PROTEOMICS-BASED ANALYSIS OF POTENTIAL SIGNATURES OF CHOLANGIOCARCINOMA

5.1 Introduction

Each living organism is built up of diverse types of molecules, the complete collections of which ("bodies") are described as "-omes", such as metabol-ome (metabolites), lipid-ome (lipids), gen-ome (DNA), tran-script-ome (RNA) and prote-ome (proteins). The study of proteomes extends beyond the question of expression (presence, absence, quantity of each protein) but also addresses cellular localization, interactions, activity, modifications and different isoforms. A large collection of different techniques can contribute to the study of proteomes, including array-based approaches and microscopic imaging, and mass spectrometry-based approaches. Mass spectrometry (MS) is a high-throughput method with the capacity to identify very small amounts proteins in complex mixtures (Aebersold et al., 2003). Since the establishment of mass spectrometry for proteome studies, the term "proteomics" largely refers to MS-based proteomics. Under optimal conditions, hundreds of individual proteins can be resolved on a single two-dimensional gel electrophoresis (2-DE), making this technology popular for studies of global proteome-scale differential expression despite a limited display of relatively abundant proteins (Elliott et al., 2009). To overcome this major limitation of 2-DE technique, we focused in quantitative proteomics that can provide insights into the dynamic changes of proteomes and aims at determining how much of each protein is present in the sample at a particular time, and how the abundances change over time. There are mainly two different approaches for protein quantification: label-based (stable isotope labeling (Ong et al., 2002) or chemical labeling (Ong et al., 2005)) and label-free approaches (Andersen et al., 2003; Ishihama et al., 2005). The advantage of label-based quantification is that proteins or peptides from multiple samples that have to be compared can be differentially labeled, mixed together and analyzed by mass

spectrometry simultaneously, minimizing the analysis time of samples. Such approaches are especially relevant to biological samples where multiple time points and/or conditions need to be evaluated.

The iTRAQ-reagent is well known for relative and absolute quantitation of proteins (Ross et al., 2004; Chong et al., 2006; Gan et al., 2007). The interest of this multiplexing reagent is that 4 or 8 analysis samples (Pierce et al., 2008) can be quantified simultaneously. In this technique, the introduction of stable isotopes using iTRAQ reagents occurs on the level of proteolytic peptides. The iTRAQ technology uses an NHS ester derivative to modify primary amino groups by linking a mass balance group (carbonyl group) and a reporter group (based on N-methylpiperazine) to proteolytic peptides via the formation of an amide bond. Due to the isobaric mass design of the iTRAQ reagents, differentially labeled peptides appear as a single peak in MS scans, reducing the probability of peak overlapping. When iTRAQ-tagged peptides are subjected to MS/MS analysis, the mass balancing carbonyl moiety is released as a neutral fragment, liberating the isotope-encoded reporter ions, which provide relative quantitative information on proteins. An inherent drawback of the reported iTRAQ technology is due to the enzymatic digestion of proteins prior to labeling, which artificially increases sample complexity. Since it has been shown that a reliable determination of protein dynamics requires quantitative evaluation of an adequate set of proteolytic peptides derived from each protein, the iTRAQ approach needs a powerful, multidimensional fractionation method of peptides before MS identification. Reported peptide separation methods include strong cation exchange (SCX) chromatography and reverse-phase chromatography (Wolters et al., 2001).

A new concept called OFFGEL electrophoresis was recently introduced with the primary aim of purifying proteins and peptides (Michel et al., 2003). This technique recovers the sample from the liquid phase and was demonstrated to be of great interest in shotgun proteomics (Burgess et al., 2006). IEF is not only a high resolution and high capacity separation method for peptides; it also provides additional physicochemical information like their isoelectric point (p*I*) (Krijgsveld et al., 2006). The p*I* value provided is used as an independent validating and filtering tool during database search for MS/MS peptide sequence identification (Cargile et al., 2004). Recently, the compatibility of iTRAQ isotope labeling and OFFGEL-IEF for

relative quantification and validation of sequence matches from database searching was shown from a BSA tryptic digest sample and complex eukaryotic samples (Lengqvist et al., 2007; Chenau et al., 2008). Surprisingly, no attempts has been done to undertake comprehensive analysis of influence of iTRAQ labeling on the proteome coverage ratio in cholangiocarcinoma (CCA), a fatal bile duct cancer which is a rare cancer worldwide but it is highly prevalent in Thailand where the liver fluke *Opisthorchis viverrini (O. viverrini)* is endemic. Diagnosis of this cancer conventionally bases on radio-imaging and tissue biopsy or serum marker confirmation. However, to date, there are no specific markers for CCA. Hence, there is an imperative need for molecular diagnostic and prognostic markers for this cancer.

Consequently in our work, we have quantitatively screened differentially expressed proteins in the human CCA cell lines and H69, a non-malignant biliary cell line. The objective of this study is to identify up- and/or down-regulated proteins of different CCA cell lines compared with H69 by employing OFFGEL, iTRAQ and LC-MS/MS technologies.

5.2 Materials and methods

5.2.1 Cell lines and cell culture

Three human CCA cell lines, namely OCA17, M156 and KKU-100 were isolated from Thai *O.verrini*-induced CCA patients and established in the Liver fluke and Cholangiocarcinoma Research Center, Khon Kaen Univeristy, Thailand. They were histologically as well, moderately and poorly differentiated adenocarcinoma, respectively. CCA cell lines were cultured in RPMI1640 medium (Gibco, Grand Island, NY, USA) containing 100 U/mL penicillin and 100 µg/mL streptomycin with 10% fetal bovine serum (Hyclone Laboratories). H69 cells, a human immortalized, non-malignant cholangiocyte cell line, were cultured as previously described (Grubman et al., 1994). Cell growth was performed at 37°C under 5% CO_2 and 95% humidified air. The presence of Mycoplasma contamination was periodically checked.

5.2.2 Patient material

Paraffin-embedded tissues were obtained by hepatic resection from the patients attending Srinagarind hospital, Khon Kaen University, Thailand. The experimental protocol was approved by the Human Research Ethics committee of Khon Kaen University (IRB No. HE42075) and prior informed patient consent were obtained in all cases.

5.2.3 iTRAQ protein sample preparation

Cells were trypsinized and washed 3 times with PBS (300 ×*g*, 5 min). Cell pellets were then lysed by a solution containing 7 M urea, 2 M thiourea, 4% (w/v) CHAPS at 4°C for 1 h using a rotary shaker. Lysis was achieved by sonication on ice (3 × 5s pulses), and the lysates were clarified by centrifugation at 14,000 ×*g* at 4°C for 15 min. Protein digestion and peptide labeling with iTRAQ reagents; protein samples were cleaned up by precipitation with 6 volumes of cold acetone at -20°C overnight followed by resuspension of pellets in 0.5 M triethyl ammonium bicarbonate (TEAB) pH 8.5 (Sigma-Aldrich) and final centrifugation step at 14,000 ×*g* at 4°C for 15 min. Proteins from supernatant were quantified with the 2-D Quant Kit (GE Healthcare, München, Germany) before diluting the protein samples up to 5 mg/ml with TEAB buffer. One-hundred µg of proteins were took for further reduction, alkylation, digestion and iTRAQ labeling using iTRAQ Reagents

Multiplex Kit (Applied Biosystems) according to manufacturer's protocol. Briefly, protein samples were reduced with 5 mM tris-(2-carboxyethyl)phosphine (TCEP) at 60°C for 1 h and the cysteine-groups were blocked using a 10 mM methyl methanethiosulfonate (MMTS) solution at room temperature for 10 min. The proteins were then digested by 10 μg of trypsin at 37°C for 16 h.

5.2.4 iTRAQ® labeling

Peptides from 100 μg of each sample were labeled with 4-plex iTRAQ® reagents according to the manufacturer's procedure (Applied BiosystemsInc. Foster City, CA). Three sets of four samples (OCA17, K100, M156 and H69) were labeled respectively with the iTRAQ® isobaric reporter tags, 114, 115, 116, and 117, respectively as shown in Figure 5.1. Labeled peptides from four samples were combined into one tube and labeling reaction stoped by evaporation in a Speed Vac to obtain to a brown pellet. A SepPac™ C18 cartridge (Waters Corporation, Milford, MA) was used to exchange the buffer, and to remove trypsin and the hydrolyzed unbound iTRAQ® reagents from the labeled peptides.

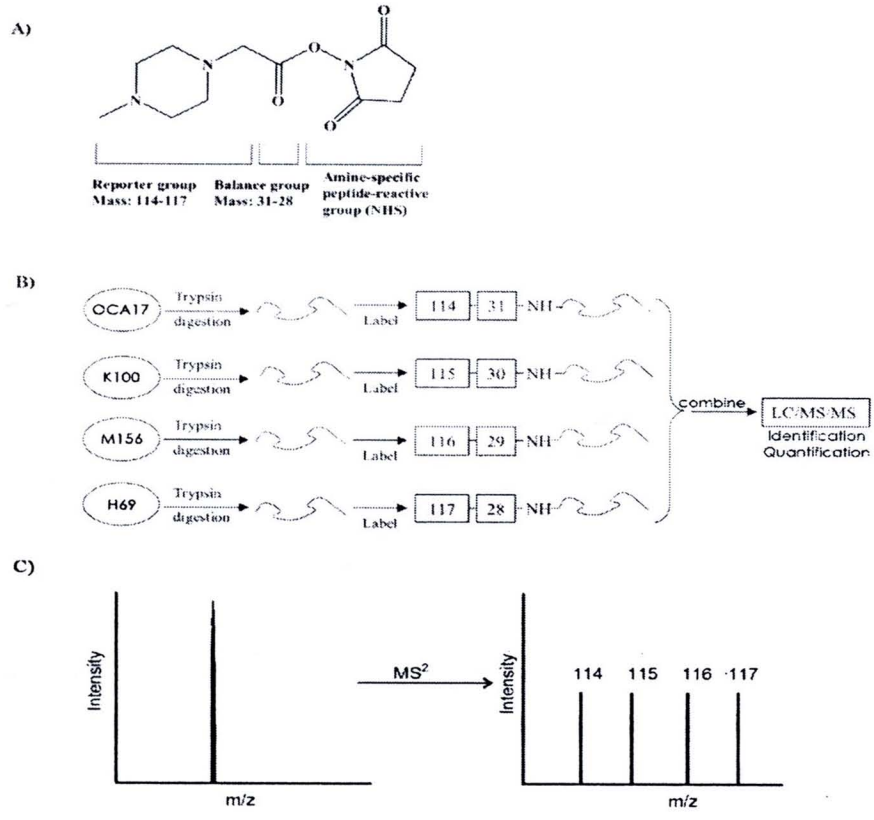

Figure 5.1 (A) Structure for reagents of isobaric tags for relative and absolute quantitation (iTRAQ), which consists of a reporter group with a mass ranging from 114 to 117 Da, a balance group with a mass ranging from 31 to 28 Da and an amine-specific peptide-reactive group. (B) Strategy for quantitation by iTRAQ. Protein mixtures from whole cell lysates of cholangiocarcinoma (CCA) cell lines and non-malignant biliary cell line H69 were digested by trypsin. The resultant peptides from OCA17, K100, M156 and H69 cells were labeled with individual iTRAQ reagents (114, 115, 116 and 117 Da), respectively. The labeled peptides were combined and analysed by liquid chromatography and mass spectrometry (LC-MS/MS) for identification and quantitation. (C) MS peaks for iTRAQ labeled peptides. The mass balance component ensured that all peptides had the same mass and hence appeared in the mass spectrum as one peak. Upon fragmentation of the peptides, the reporter components were released and the intensities of these reporter ions could be used to estimate protein quantities.

5.2.5 Peptide OFFGEL fractionation

For p*I*-based peptide separation, we used the 3100 OFF-GEL Fractionator (Agilent Technologies, Böblingen, Germany) with a 24-well set-up. Prior to electrofocusing, samples were desalted onto a Sep-Pak C18 cartridge (Waters). For 24-well set-up, peptide samples were dilute to a final volume of respectively 3.6 ml using OFFGEL peptide sample solution. To start, the IPG gel strips of 24 cm-long (GE Healthcare, München, Germany) with a 3-10 linear pH range were rehydrated with the Peptide IPG Strip Rehydradation Solution according to the protocol of the manufacturer for 15 min. Then, 150 µl of sample was loaded in each well. Electrofocusing of the peptides is performed at 20°C and 50 µA until the 50 kVh level was reached. After focusing, the 24-peptide fractions were withdrawn and the wells rinsed with 200 µL of a solution of water/methanol/formic acid (49/50/1) after 15 min, the rinsing solutions were pooled with their corresponding peptide fraction. All fractions were evaporated by centrifugation under vacuum and maintained at -20°C. Just prior to the nano-LC, the fractions were resuspended in 20 µl of H_2O with 0.1% (v/v) trifluoroacetic acid (TFA).

5.2.6 Capillary LC separation and LC-MS/MS analysis

The samples were separated on an Ultimate 3,000 nano- LC system (Dionex, Sunnyvale, USA) using a C18 column (PepMap100, 3 µm, 100A, 75 µm id × 15 cm, Dionex) at a flow rate of 300 nanoliter/min. Buffer A was 2% ACN in water with 0.05% TFA and buffer B was 80% ACN in water with 0.04% TFA. Peptides were desalted for 3 min. using only buffer A on the precolumn, followed by a separation for 60 min. using the following gradient: 0 to 20% B in 10 min, 20% to 55% B in 45 min and 55% to 100% B in 5 min. Chromatograms were recorded at the wavelength of 214 nm. Peptide fractions were collected using a Probot microfraction collector (Dionex). Product ion spectra were collected in an information-dependent acquisition (IDA) mode. IDA mode settings included continuous cycles of one full-scan TOF MS from m/z 400 to 1,100 (1.5 sec) plus four-product ion scans from m/z 100 to 1,400 (3 sec each). Precursor m/z values were selected from a peak list automatically generated by Analyst QS software (Applied Biosystems) from the TOF-MS scan during acquisition, starting with the most intense ion.

5.2.7 Peptide and protein identification and database searches

Peptide and protein identification were performed by the ProteinPilotTM Soft- ware V 2.0 (Applied Biosystems) using the Paragon algorithm (Shilov et al., 2007). Each MS/MS spectrum was searched for *Homo sapiens* against the Swissprot database (16 Sep 2010). The searches were run using with the fixed modification of methylmethanethiosulfate labeled cysteine parameter enabled. Other parameters such as tryptic cleavage specificity, precursor ion mass accuracy and fragment ion mass accuracy are MALDI 4800 built-in functions of ProteinPilot software. The ProteinPilot Software calculates a confidence percentage (the unused score) that reflects the probability that the hit is a false positive, meaning that at 95% CI level, there is a false positive identification chance of about 5%. While this software automatically accepts all peptides having an identification confidence level >1%, only proteins having at least one peptide above 95% confidence were initially recorded.

Rates of false identifications were estimated using a concatenated reversed sequence database (Elias et al., 2007). The low confidence peptides cannot give positive protein identification by themselves, but may support the presence of a protein identified using other peptides with higher confidence. Performing the search against a concatenated database containing both forward and reversed sequences allowed estimation of the false discovery rate below 1%. The experimental p*I* for each peptide was calculated using a p*I*/*Mr* tool of the ExPASy Proteomic Server (Gasteiger et al., 2003).

5.2.8 Classification of iTRAQ identified proteins

The relative abundance of each peptide was determined by ProteinPilot™ using the peak areas of signature ions from the iTRAQ®-labeled peptides. The Pro-group™ Algorithm within the ProteinPilot™ version 2.0 software was used to compile the peptide identification into protein groups and to show protein-based ratios of relative abundance. Peptides shared among related but distinct proteins were not used for quantitation. Peptide MS/MS for protein identifications inferred from single peptide hits were manually inspected. In all cases except two, protein identifications made from single peptide hits in one-depletion experiment were made with two or more peptides in at least one of the alternative depletion

experiments. Proteins were considered over- and under-expressed in three CCA cell lines relative to non-cancer control cell line if the iTRAQ® ratio of C/N was >1.6 and < 0.6, respectively. Additionally, the acceptable corresponding N/N ratio was between 0.8 and 1.2 in at least one experiment (Boylan et al., 2010).

5.2.9 Immunohistochemistry

Immunohistochemical (IHC) reactions were performed on 4 μm-thick sections of TMA silane-coated slides (Sigma, St. Louis, MO, USA) by an immunoperoxidase method as previously described (Yonglitthipagon et al., 2010). The sections probed with rabbit polyclonal anti-delta cathenin (ab72039, Abcam Inc., USA) diluted 1:300 (v/v) or mouse monoclonal anti-cathepsin D (ab6313, Abcam) diluted 1:300 (v/v) or mouse polyclonal anti-transgelin 3 (12246-1-AP, ProteinTech, USA) diluted 1:100 (v/v) in PBS and incubated overnight at 4°C. After rinsing for 3 × 5 min with PBS the sections were incubated with biotin-conjugated goat anti-rabbit immunoglobulin (Zymed Labs., San Francisco, CA) diluted 1:300 (v/v) or HRP-conjugated goat anti-mouse IgG (Abcam) diluted 1:300 (v/v) in PBS and incubated at RT for 1 h. The sections were then incubated with a horseradish peroxidase-conjugated streptavidin (Zymed Labs.) diluted 1:300 (v/v) in PBS at RT for 1 h for ABC system. Sections were rinsed with PBS for 2 × 10 min, after which the sections were developed with DAB (Sigma Chemical Co.). The sections were counterstained with Mayer's haematoxylin, dehydrated, cleared in xylene and mounted in Permount®.

5.3 Results

5.3.1 Significant differentially regulated proteins

To identify cholangiocarcinoma-associated proteins, we compared whole cell lysates obtained from CCA cell lines and non-tumor biliary cell line. The complexity of our samples were prior decreased by using OFFGEL and resultant whole cell lysate proteomes from OCA17, M156, K100 and H69 were labeled with iTRAQ reagents separately, and mixed samples were analyzed by nano-LC-MS/MS. The estimation (and calculation) of the relative quantitative ratio from an iTRAQ experiment was reported earlier (Gan et al., 2007), only peptides above or equal to a 99% confidence were taken into consideration in addition to the default peptide

selection criteria. A total of 628 proteins were identified with ≥99% confidence from 89,319 possible identified peptides. More than 90% of the identified proteins were identified with at least two MS/MS spectra. Using the concatenated target-decoy database search strategy as detailed by Elias and Gygi (Elias et al., 2007), a 1% rate of local false discovery was estimated, which further strengthened the reliability of the data. Based on the peptide selection criteria pre-set in ProteinPilot V.2.0 software, all peptides were used for quantitation, except peptides without an iTRAQ modification or reporter ions (i.e., no quantitation): peptide with low intensity ratio, i.e., a total area count less than 40; shared peptides between similar protein isoforms; peptides derived from the same MS/MS spectrum window; and peptides with a confidence below 0.5%. Based on all these criteria, 628 out of 680 total proteins (92.35%) gave at least one relative quantitative ratio in either 114:117, 115:117 and 116:117. Additionally, to allow analytical triplicate measurements, the experiment was set up in a triplex fashion as shown in Table 5.1.

Table 5.1 Summary of the number of proteins identified in whole cell lysates of CCA and H69 cell lines

Batch	iTRAQ Mass Tag				Confidence level		UP[a]	DP[b]
	114	115	116	117	≥99%	≥95%		
1	OCA17	K100	M156	H69	628	644	201	31
2	K100	M156	H69	OCA17		in process		
3	M156	H69	OCA17	K100		in process		

Note:[a]Up-regulated proteins and [b]Down-regulated proteins.

Furthermore, it has been reported that peptides with a quantitation ratio of 9999, 0, or blank can sometimes be a true observation as a result of intrinsic biological effects (Glen et al., 2008). In the result, however, none of the peptides showed a quantitative value of 0 and 999, and all the values were either unsustained or statistically insignificant as a result of intrinsic biological effects. Among 628 non-redundantly identified proteins from 24 OFFGEL fractions, 201 proteins were increased more than 1.6-fold (Table 5.2) and 31 proteins were decreased less than 0.6-fold (Table 5.3) in the whole cell lysates of CCA cell lines compared with H69.

5.3.2 Protein classifications

These 628 proteins, which were differentially expressed between CCA cells and H69, could be classified into 10 categories for cellular components using the PANTER classification system (Figure 5.2). A majority of proteins identified (39%) were classified as extracellular (23%) or membrane (16%) proteins. Other identified proteins were classified as intracellular (50%), whereas 11% were unclassified. Of the 628 significantly differentially expressed proteins, some of these were classified into biological processes previously associated with cancer progression, such as carbohydrate metabolism, cell cycle, cell structure and motility, cell proliferation, and differentiation (Ernoult et al., 2010; Hu et al., 2010).

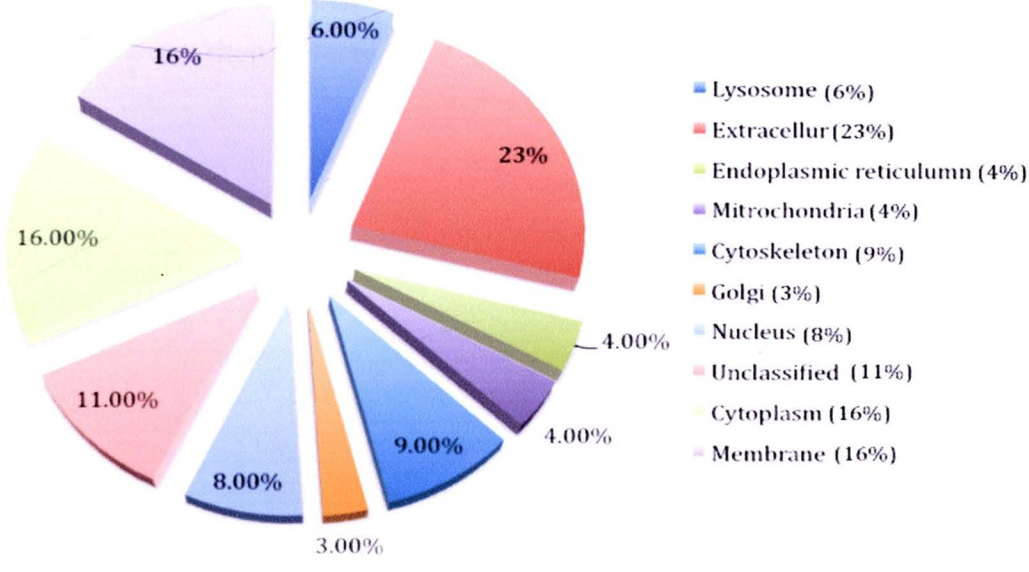

Figure 5.2 Pie chart showing various cellular compartments as a percentage of the 628 differentially expressed proteins based on the PANTHER classification system.

5.3.3 iTRAQ analysis of differentially expressed proteins

As expected, significant over-expression of several proteins have been reported to associate with tumor initiation and progression in many cancers. From the list of proteins identified to have up-regulation in CCA cell lines compared to a control H69, candidate biomarkers were selected for further verification based on the literature searches through the U.S. National Library of Medicine National Institutes of Health (http://www.ncbi.nlm.nih.gov/pubmed) to determine whether these proteins are novel molecules that have yet to be explored as potential biomarkers in CCA and whether these proteins are known to participate in critical pathways implicated in cancer initiation and progression. With these criteria, transgelin 3 (TAGL3), catenin delta-1 (CTND1) and cathepsin-D (CATD) in which highly elevated in CCA cell lines (17.8, 7.7 and 6.73 fold higher than H69, respectively) were then selected for further immunolocalization by IHC in CCA tissues.

Table 5.2 Summary of identified proteins that were increased in CCA cell lines

No.	Accession No.[a]	Description	WD:N[b]	PD:N[c]	MD:N[d]
1	sp|P04264|K2C1_HUMAN	Keratin, type II cytoskeletal 1	23.9	24.8	21.4
2	sp|Q9UI15|TAGL3_HUMAN	Transgelin-3	25.4	19.0	19.0
3	sp|O14556|G3PT_HUMAN	Glyceraldehyde-3-phosphate dehydrogenase	19.4	16.4	19.9
4	sp|O60716|CTND1_HUMAN	Catenin delta-1	8.8	7.4	6.9
5	sp|P08727|K1C19_HUMAN	Keratin, type I cytoskeletal 19	8.2	8.3	6.4
6	sp|P07339|CATD_HUMAN	Cathepsin D	7.8	6.5	5.9
7	sp|Q12931|TRAP1_HUMAN	Heat shock protein 75 kDa, mitochondrial	7.7	5.7	6.9
8	sp|Q9Y2X3|NOP58_HUMAN	Nucleolar protein 58	6.0	9.1	4.4
9	sp|P07864|LDHC_HUMAN	L-lactate dehydrogenase C chain	6.2	6.0	6.1
10	sp|Q9Y6N5|SQRD_HUMAN	Sulfide:quinoneoxidoreductase, mitochondrial	5.8	6.0	5.5
11	sp|P52209|6PGD_HUMAN	6-phosphogluconate dehydrogenase, decarboxylating	6.5	6.4	4.3
12	sp|P62910|RL32_HUMAN	60S ribosomal protein L32	5.4	6.4	4.8
13	sp|P21912|DHSB_HUMAN	Succinatedehydrogenase	5.2	5.4	5.6
14	sp|Q96C86|DCPS_HUMAN	Scavenger mRNA-decapping enzyme DcpS	5.0	6.7	4.4
15	sp|P16104|H2AX_HUMAN	Histone H2A.x	5.3	5.2	5.6
16	sp|P13929|ENOB_HUMAN	Beta-enolase	5.7	4.8	5.3
17	sp|O60218|AK1BA_HUMAN	Aldo-ketoreductase family 1 member B10	4.4	5.3	5.7
18	sp|Q13162|PRDX4_HUMAN	Peroxiredoxin-4	5.4	4.8	4.7
19	sp|Q9HAW9|UD18_HUMAN	UDP-glucuronosyl transferase 1-8	4.3	5.1	5.3
20	sp|P62820|RAB1A_HUMAN	Ras-related protein Rab-1A	5.2	4.0	5.0
21	sp|Q6KB66|K2C80_HUMAN	Keratin, type II cytoskeletal 80	5.1	4.4	3.8
22	sp|P05787|K2C8_HUMAN	Keratin, type II cytoskeletal 8	4.2	4.7	4.1
23	sp|P07602|SAP_HUMAN	Proactivator polypeptide	4.2	4.6	4.1
24	sp|P51553|IDH3G_HUMAN	Isocitrate dehydrogenase [NAD] subunit gamma	4.4	5.1	3.3
25	sp|P55769|NH2L1_HUMAN	NHP2-like protein 1	4.3	4.5	3.9
26	sp|P05387|RLA2_HUMAN	60S acidic ribosomal protein P2	4.4	4.3	3.6
27	sp|P05783|K1C18_HUMAN	Keratin, type I cytoskeletal 18	4.0	4.3	3.9
28	sp|Q16629|SFRS7_HUMAN	Splicing factor, arginine/serine-rich 7	4.7	4.0	3.3
29	sp|P35580|MYH10_HUMAN	Myosin-10	3.7	3.9	4.2
30	sp|P42574|CASP3_HUMAN	Caspase-3	3.8	4.2	3.5
31	sp|P46782|RS5_HUMAN	40S ribosomal protein S5	3.5	4.6	3.3
32	sp|Q96QK1|VPS35_HUMAN	Vacuolar protein sorting-associated protein 35	3.9	4.2	3.4
33	sp|P04844|RPN2_HUMAN	Dolichyl-diphospho-oligosaccharide	3.6	3.7	3.7
34	sp|P84103|SFRS3_HUMAN	Splicing factor, arginine/serine-rich 3	3.9	3.6	3.5
35	sp|Q9Y3A5|SBDS_HUMAN	Ribosome maturation protein SBDS	3.6	4.7	2.7

Table 5.2 Summary of identified proteins that were increased in CCA cell lines (Cont.)

No.	Accession No.[a]	Description	WD:N[b]	PD:N[c]	MD:N[d]
36	sp|Q07955|SFRS1_HUMAN	Splicing factor, arginine/serine-rich 1	3.2	4.3	3.5
37	sp|Q00325|MPCP_HUMAN	Phosphate carrier protein, mitochondrial	3.5	4.6	2.9
38	sp|P27695|APEX1_HUMAN	DNA-(apurinic or apyrimidinic site) lyase	2.8	4.0	3.7
39	sp|P21796|VDAC1_HUMAN	Voltage-dependent anion-selective channel protein 1	3.4	3.6	3.5
40	sp|P56192|SYMC_HUMAN	Methionyl-tRNA synthetase, cytoplasmic	3.3	4.0	3.2
41	sp|P49773|HINT1_HUMAN	Histidine triad nucleotide-binding protein 1	3.7	3.6	3.0
42	sp|P52272|HNRPM_HUMAN	Heterogeneous nuclear ribonucleoprotein M	3.6	3.5	3.2
43	sp|Q15102|PA1B3_HUMAN	Platelet-activating factor acetylhydrolase IB	3.9	3.1	3.2
44	sp|Q8NC51|PAIRB_HUMAN	Plasminogen activator inhibitor 1 RNA-binding protein	3.1	3.8	3.1
45	sp|Q99584|S10AD_HUMAN	Protein S100-A13	3.2	2.8	4.0
46	sp|P05141|ADT2_HUMAN	ADP/ATP translocase 2	3.0	3.7	3.1
47	sp|Q99623|PHB2_HUMAN	Prohibitin-2	2.7	3.6	3.5
48	sp|P49591|SYSC_HUMAN	Seryl-tRNAsynthetase, cytoplasmic	2.9	2.8	4.0
49	sp|P48735|IDHP_HUMAN	Isocitratedehydrogenase [NADP], mitochondrial	3.0	3.3	3.2
50	sp|Q09666|AHNK_HUMAN	Neuroblast differentiation-associated protein AHNAK	3.5	2.7	3.2
51	sp|P35354|PGH2_HUMAN	Prostaglandin G/H synthase 2	2.4	2.8	4.3
52	sp|P63220|RS21_HUMAN	40S ribosomal protein S21	3.6	3.0	2.8
53	sp|P63244|GBLP_HUMAN	Guanine nucleotide-binding protein subunit beta-2-like 1	3.3	3.0	3.0
54	sp|Q9Y5K5|UCHL5_HUMAN	Ubiquitin carboxyl-terminal hydrolaseisozyme L5	3.8	3.1	2.2
55	sp|O43175|SERA_HUMAN	D-3-phosphoglycerate dehydrogenase	2.8	3.0	3.1
56	sp|P05023|AT1A1_HUMAN	Sodium/potassium-transporting ATPase subunit alpha-1	2.9	3.3	2.6
57	sp|Q9UL25|RAB21_HUMAN	Ras-related protein Rab-21	2.8	3.6	2.4
58	sp|P30043|BLVRB_HUMAN	Flavinreductase	3.7	2.4	2.7
59	sp|P39656|OST48_HUMAN	Dolichyl-diphosphooligosaccharide-48 kDa	2.8	2.8	3.2
60	sp|P46939|UTRO_HUMAN	Utrophin	2.0	4.3	2.2
61	sp|P55263|ADK_HUMAN	Adenosine kinase	2.8	2.6	3.1
62	sp|P27708|PYR1_HUMAN	CAD protein	2.9	2.7	2.9
63	sp|Q9Y277|VDAC3_HUMAN	Voltage-dependent anion-selective channel protein 3	3.0	2.6	2.9
64	sp|P49411|EFTU_HUMAN	Elongation factor Tu, mitochondrial	2.9	2.8	2.6
65	sp|P39023|RL3_HUMAN	60S ribosomal protein L3	2.7	3.1	2.5
66	sp|P08134|RHOC_HUMAN	Rho-related GTP-binding protein RhoC	2.9	2.8	2.5

Table 5.2 Summary of identified proteins that were increased in CCA cell lines (Cont.)

No.	Accession No.[a]	Description	WD:N[b]	PD:N[c]	MD:N[d]
67	sp|Q16822|PCKGM_HUMAN	Phosphoenolpyruvatecarboxykinase [GTP]	2.7	2.8	2.8
68	sp|P31930|QCR1_HUMAN	Cytochrome b-c1 complex subunit 1	2.3	3.4	2.5
69	sp|P06748|NPM_HUMAN	Nucleophosmin	2.9	2.8	2.3
70	sp|P45880|VDAC2_HUMAN	Voltage-dependent anion-selective channel protein 2	3.0	2.3	2.7
71	sp|Q6NUK1|SCMC1_HUMAN	Calcium-binding mitochondrial carrier protein SCaMC-1	2.7	2.6	2.6
72	sp|P07741|APT_HUMAN	Adenine phosphoribosyltransferase	3.0	2.5	2.3
73	sp|P41091|IF2G_HUMAN	Eukaryotic translation initiation factor 2 subunit 3	2.6	2.5	2.7
74	sp|P08243|ASNS_HUMAN	Asparaginesynthetase [glutamine-hydrolyzing]	2.3	2.3	3.0
75	sp|P21281|VATB2_HUMAN	V-type proton ATPase subunit B, brain isoform	2.2	3.6	1.9
76	sp|P46783|RS10_HUMAN	40S ribosomal protein S10	2.7	2.4	2.5
77	sp|P35232|PHB_HUMAN	Prohibitin	2.1	2.7	2.7
78	sp|P39019|RS19_HUMAN	40S ribosomal protein S19	2.5	2.7	2.4
79	sp|Q06830|PRDX1_HUMAN	Peroxiredoxin-1	2.7	2.4	2.5
80	sp|P06576|ATPB_HUMAN	ATP synthase subunit beta, mitochondrial	2.5	2.7	2.3
81	sp|P25398|RS12_HUMAN	40S ribosomal protein S12	2.6	2.5	2.4
82	sp|Q13885|TBB2A_HUMAN	Tubulin beta-2A chain	2.4	2.5	2.5
83	sp|O75390|CISY_HUMAN	Citrate synthase, mitochondrial	2.3	2.9	2.2
84	sp|P68400|CSK21_HUMAN	Casein kinase II subunit alpha	2.5	2.3	2.6
85	sp|Q86VP6|CAND1_HUMAN	Cullin-associated NEDD8-dissociated protein 1	2.4	2.5	2.5
86	sp|P15880|RS2_HUMAN	40S ribosomal protein S2	2.2	2.7	2.5
87	sp|P17931|LEG3_HUMAN	Galectin-3	2.0	2.7	2.5
88	sp|P34897|GLYM_HUMAN	Serine hydroxymethyl transferase, mitochondrial	2.1	2.6	2.5
89	sp|P14868|SYDC_HUMAN	Aspartyl-tRNAsynthetase, cytoplasmic	2.3	2.4	2.4
90	sp|P46940|IQGA1_HUMAN	RasGTPase-activating-like protein IQGAP1	2.2	2.4	2.5
91	sp|Q15365|PCBP1_HUMAN	Poly(rC)-binding protein 1	2.3	2.5	2.2
92	sp|P38117|ETFB_HUMAN	Electron transfer flavoprotein subunit beta	2.3	2.5	2.2
93	sp|P23396|RS3_HUMAN	40S ribosomal protein S3	2.3	2.4	2.3
94	sp|P62942|FKB1A_HUMAN	Peptidyl-prolylcis-transisomerase FKBP1A	2.8	2.0	2.2
95	sp|P22087|FBRL_HUMAN	rRNA 2'-O-methyltransferase fibrillarin	2.3	2.6	2.0
96	sp|P36957|ODO2_HUMAN	Dihydrolipoyllysine-residue succinyltransferase	2.4	2.0	2.6
97	sp|P17844|DDX5_HUMAN	Probable ATP-dependent RNA helicase DDX5	2.3	2.4	2.2
98	sp|Q96I99|SUCB2_HUMAN	Succinyl-CoAligase [GDP-forming] subunit beta	1.9	2.6	2.4

Table 5.2 Summary of identified proteins that were increased in CCA cell lines (Cont.)

No.	Accession No.[a]	Description	WD:N[b]	PD:N[c]	MD:N[d]
99	sp|P38646|GRP75_HUMAN	Stress-70 protein, mitochondrial	2.5	2.2	2.2
100	sp|P14618|KPYM_HUMAN	Pyruvatekinaseisozymes M1/M2	2.3	2.2	2.4
101	sp|P08708|RS17_HUMAN	40S ribosomal protein S17	2.2	2.4	2.2
102	sp|P51665|PSD7_HUMAN	26S proteasome non-ATPase regulatory subunit 7	2.3	2.2	2.3
103	sp|Q00341|VIGLN_HUMAN	Vigilin	2.5	1.7	2.6
104	sp|P02545|LMNA_HUMAN	Lamin-A/C	2.2	2.1	2.5
105	sp|P62244|RS15A_HUMAN	40S ribosomal protein S15a	2.0	2.6	2.1
106	sp|P62273|RS29_HUMAN	40S ribosomal protein S29	2.4	2.3	2.0
107	sp|P26641|EF1G_HUMAN	Elongation factor 1-gamma	2.3	2.2	2.3
108	sp|P22033|MUTA_HUMAN	Methylmalonyl-CoAmutase, mitochondrial	2.2	2.4	2.1
109	sp|P61970|NTF2_HUMAN	Nuclear transport factor 2	2.4	2.8	1.5
110	sp|P62937|PPIA_HUMAN	Peptidyl-prolylcis-transisomerase A	2.7	2.1	1.9
111	sp|P62266|RS23_HUMAN	40S ribosomal protein S23	2.3	2.2	2.2
112	sp|P31939|PUR9_HUMAN	Bifunctionalpurine biosynthesis protein PURH	2.3	2.2	2.2
113	sp|P61353|RL27_HUMAN	60S ribosomal protein L27	2.2	2.5	1.9
114	sp|P62829|RL23_HUMAN	60S ribosomal protein L23	2.0	2.3	2.3
115	sp|P09622|DLDH_HUMAN	Dihydrolipoyl dehydrogenase	2.2	3.0	1.5
116	sp|Q15181|IPYR_HUMAN	Inorganic pyrophosphatase	2.3	1.9	2.4
117	sp|P62701|RS4X_HUMAN	40S ribosomal protein S4, X isoform	2.1	2.4	2.0
118	sp|P09429|HMGB1_HUMAN	High mobility group protein B1	2.0	2.1	2.3
119	sp|P30048|PRDX3_HUMAN	Thioredoxin-dependent peroxide reductase	2.2	2.6	1.7
120	sp|P17987|TCPA_HUMAN	T-complex protein 1 subunit alpha	2.4	2.1	2.0
121	sp|P11172|PYR5_HUMAN	Uridine 5'-monophosphate synthase	2.2	2.1	2.2
122	sp|P55884|EIF3B_HUMAN	Eukaryotic translation initiation factor 3 subunit B	2.3	2.1	2.1
123	sp|Q99832|TCPH_HUMAN	T-complex protein 1 subunit Beta	2.1	2.3	2.0
124	sp|P12268|IMDH2_HUMAN	Inosine-5'-monophosphate dehydrogenase 2	2.2	2.2	1.9
125	sp|O00410|IPO5_HUMAN	Importin-5	2.1	1.8	2.4
126	sp|P35237|SPB6_HUMAN	Serpin B6	1.9	2.1	2.4
127	sp|Q9NSD9|SYFB_HUMAN	Phenylalanyl-tRNAsynthetase beta chain	2.3	1.8	2.1
128	sp|Q9Y383|LC7L2_HUMAN	Putative RNA-binding protein Luc7-like 2	2.1	2.8	1.4
129	sp|Q92769|HDAC2_HUMAN	Histonedeacetylase 2	2.1	2.0	2.1
130	sp|P40227|TCPZ_HUMAN	T-complex protein 1 subunit zeta	1.7	2.3	2.2
131	sp|O15523|DDX3Y_HUMAN	ATP-dependent RNA helicase DDX3Y	1.8	2.2	2.1
132	sp|Q15008|PSMD6_HUMAN	26S proteasome non-ATPase regulatory subunit 6	2.1	1.9	2.2

Table 5.2 Summary of identified proteins that were increased in CCA cell lines (Cont.)

No.	Accession No.[a]	Description	WD:N[b]	PD:N[c]	MD:N[d]
133	sp|Q13200|PSMD2_HUMAN	26S proteasome non-ATPase regulatory subunit 2	1.8	2.1	2.2
134	sp|P61088|UBE2N_HUMAN	Ubiquitin-conjugating enzyme E2 N	2.0	2.5	1.5
135	sp|Q15149|PLEC1_HUMAN	Plectin-1	2.0	1.9	2.2
136	sp|P62750|RL23A_HUMAN	60S ribosomal protein L23a	1.6	2.4	2.1
137	sp|P22392|NDKB_HUMAN	Nucleoside diphosphatekinase B	2.2	2.0	1.8
138	sp|P22234|PUR6_HUMAN	Multifunctional protein ADE2	2.2	1.8	2.0
139	sp|Q96AG4|LRC59_HUMAN	Leucine-rich repeat-containing protein 59	1.8	2.1	2.1
140	sp|P68366|TBA4A_HUMAN	Tubulin alpha-4A chain	2.2	1.6	2.2
141	sp|P62140|PP1B_HUMAN	Serine/threonine-protein phosphatase PP1	2.3	1.9	1.7
142	sp|Q9UQ80|PA2G4_HUMAN	Proliferation-associated protein 2G4	1.7	2.7	1.6
143	sp|Q08211|DHX9_HUMAN	ATP-dependent RNA helicase A	1.8	2.0	2.1
144	sp|P13639|EF2_HUMAN	Elongation factor 2	2.2	1.9	1.8
145	sp|P07355|ANXA2_HUMAN	Annexin A2	1.8	1.9	2.1
146	sp|P50991|TCPD_HUMAN	T-complex protein 1 subunit delta	2.1	1.8	2.0
147	sp|P25705|ATPA_HUMAN	ATP synthase subunit alpha, mitochondrial	1.8	2.1	1.9
148	sp|P08865|RSSA_HUMAN	40S ribosomal protein SA	1.9	2.1	1.8
149	sp|P84077|ARF1_HUMAN	ADP-ribosylation factor 1	1.8	1.9	2.1
150	sp|Q14152|EIF3A_HUMAN	Eukaryotic translation initiation factor 3 subunit A	2.0	1.9	1.8
151	sp|P54886|P5CS_HUMAN	Delta-1-pyrroline-5-carboxylate synthase	1.8	2.2	1.8
152	sp|O00303|EIF3F_HUMAN	Eukaryotic translation initiation factor 3 subunit F	1.7	1.8	2.2
153	sp|Q00839|HNRPU_HUMAN	Heterogeneous nuclear ribonucleoprotein U	2.1	1.8	1.8
154	sp|Q02218|ODO1_HUMAN	2-oxoglutarate dehydrogenase, mitochondrial	2.2	1.6	1.9
155	sp|P84085|ARF5_HUMAN	ADP-ribosylation factor 5	2.1	1.7	1.9
156	sp|P05386|RLA1_HUMAN	60S acidic ribosomal protein P1	1.9	2.0	1.8
157	sp|P61978|HNRPK_HUMAN	Heterogeneous nuclear ribonucleoprotein K	2.2	1.8	1.7
158	sp|P00505|AATM_HUMAN	Aspartateaminotransferase, mitochondrial	1.9	2.0	1.8
159	sp|P37802|TAGL2_HUMAN	Transgelin-2	2.2	1.7	1.6
160	sp|P40926|MDHM_HUMAN	Malatedehydrogenase, mitochondrial	2.1	1.7	1.8
161	sp|P36578|RL4_HUMAN	60S ribosomal protein L4	1.8	2.1	1.7
162	sp|P46777|RL5_HUMAN	60S ribosomal protein L5	1.8	2.0	1.7
163	sp|O00299|CLIC1_HUMAN	Chloride intracellular channel protein 1	2.1	1.6	1.8
164	sp|Q15029|U5S1_HUMAN	116 kDa U5 small nuclear ribonucleoprotein component	2.2	1.6	1.6

Table 5.2 Summary of identified proteins that were increased in CCA cell lines (Cont.)

No.	Accession No.[a]	Description	WD:N[b]	PD:N[c]	MD:N[d]
165	sp|P34932|HSP74_HUMAN	Heat shock 70 kDa protein 4	1.8	1.8	1.8
166	sp|Q12904|AIMP1_HUMAN	AminoacyltRNAsynthase complex	1.7	2.2	1.5
167	sp|P62195|PRS8_HUMAN	26S protease regulatory subunit 8	2.1	1.7	1.6
168	sp|P54136|SYRC_HUMAN	Arginyl-tRNAsynthetase, cytoplasmic	1.7	1.7	1.9
169	sp|P26599|PTBP1_HUMAN	Polypyrimidine tract-binding protein 1	2.0	1.8	1.6
170	sp|P60891|PRPS1_HUMAN	Ribose-phosphate pyrophosphokinase 1	2.0	1.7	1.7
171	sp|P05388|RLA0_HUMAN	60S acidic ribosomal protein P0	1.7	1.9	1.6
172	sp|O75369|FLNB_HUMAN	Filamin-B	2.0	1.6	1.6
173	sp|P58876|H2B1D_HUMAN	Histone H2B type 1-D	1.8	1.7	1.8
174	sp|P60866|RS20_HUMAN	40S ribosomal protein S20	1.8	1.7	1.7
175	sp|O00231|PSD11_HUMAN	26S proteasome non-ATPase regulatory subunit 11	1.7	1.9	1.6
176	sp|P20618|PSB1_HUMAN	Proteasome subunit beta type-1	2.0	1.6	1.6
177	sp|P39687|AN32A_HUMAN	Acidic leucine-rich nuclear phosphoprotein 32	1.8	1.7	1.6
178	sp|Q14166|TTL12_HUMAN	Tubulin—tyrosine ligase-like protein 12	1.7	2.0	1.5
179	sp|P47897|SYQ_HUMAN	Glutaminyl-tRNAsynthetase	2.2		2.9
180	sp|Q96FW1|OTUB1_HUMAN	Ubiquitinthioesterase OTUB1	1.7	1.9	1.5
181	sp|Q14204|DYHC1_HUMAN	Cytoplasmicdynein 1 heavy chain 1	1.6	1.7	1.7
182	sp|P68104|EF1A1_HUMAN	Elongation factor 1-alpha 1	1.8	1.7	1.6
183	sp|Q13283|G3BP1_HUMAN	RasGTPase-activating protein-binding protein 1	1.9	1.7	1.5
184	sp|Q15185|TEBP_HUMAN	Prostaglandin E synthase 3	1.5	2.1	1.5
185	sp|P07910|HNRPC_HUMAN	Heterogeneous nuclear ribonucleoproteins C1/C2	1.8	1.4	1.8
186	sp|P60842|IF4A1_HUMAN	Eukaryotic initiation factor 4A-I	1.7	1.6	1.7
187	sp|P67870|CSK2B_HUMAN	Casein kinase II subunit beta	1.7	1.4	1.9
188	sp|Q15907|RB11B_HUMAN	Ras-related protein Rab-11B	1.8	1.7	1.5
189	sp|P27348|1433T_HUMAN	14-3-3 protein theta	1.8	1.6	1.6
190	sp|P33176|KINH_HUMAN	Kinesin-1 heavy chain	1.7	2.4	0.9
191	sp|P04083|ANXA1_HUMAN	Annexin A1	1.9	1.5	1.6
192	sp|P62851|RS25_HUMAN	40S ribosomal protein S25	1.6	1.8	1.5
193	sp|P20700|LMNB1_HUMAN	Lamin-B1	1.7	1.5	1.7
194	sp|P31948|STIP1_HUMAN	Stress-induced-phosphoprotein 1	1.7	1.5	1.7
195	sp|P13797|PLST_HUMAN	Plastin-3	1.7	1.4	1.9
196	sp|P12814|ACTN1_HUMAN	Alpha-actinin-1	1.9	1.3	1.7
197	sp|P55209|NP1L1_HUMAN	Nucleosome assembly protein 1-like 1	1.5	2.1	1.2
198	sp|P62269|RS18_HUMAN	40S ribosomal protein S18	1.6	1.8	1.4

Table 5.2 Summary of identified proteins that were increased in CCA cell lines (Cont.)

No.	Accession No.[a]	Description	WD:N[b]	PD:N[c]	MD:N[d]
199	sp|P49368|TCPG_HUMAN	T-complex protein 1 subunit gamma	1.6	1.6	1.6
200	sp|P52597|HNRPF_HUMAN	Heterogeneous nuclear ribonucleoprotein F	1.5	2.5	0.8
201	sp|P62826|RAN_HUMAN	GTP-binding nuclear protein Ran	1.7	1.6	1.5

Note: Only proteins in the CCA cell lines compared with H69 and have ≥ 1.6-fold change were collected in this table. [a]Websites to access the data to the listed proteins: http://www.ncbi.nlm.nih.gov. [b]WD:N, [c]PD:N and [d]MD:N correspond to intensity ratio of OCA17:H69, K100:H69 and M156:H69, respectively. OCA17, well differentiated adenocarcinoma cell line; M156, moderately differentiated adenocarcinoma cell line; K100, poorly differentiated adenocarcinoma cell line; H69, non-malignant biliary cell line.

Table 5.3 Summary of identified proteins that were decreased in CCA cell lines

No.	Accession No.[a]	Description	WD:N[b]	PD:N[c]	MD:N[d]
1	sp|P14550|AK1A1_HUMAN	Alcohol dehydrogenase [NADP+]	0.5875	0.6268	0.5695
2	sp|P27797|CALR_HUMAN	Calreticulin	0.5262	0.5128	0.7115
3	sp|P22061|PIMT_HUMAN	Protein-L-isoaspartate (D-aspartate) O-methyltransferase	0.4793	0.5626	0.6903
4	sp|P18669|PGAM1_HUMAN	Phosphoglyceratemutase 1	0.5282	0.563	0.6132
5	sp|P16949|STMN1_HUMAN	Stathmin	0.7738	0.459	0.4622
6	sp|Q92841|DDX17_HUMAN	Probable ATP-dependent RNA helicase DDX17	0.6107	0.555	0.4996
7	sp|Q12906|ILF3_HUMAN	Interleukin enhancer-binding factor 3	0.642	0.5205	0.481
8	sp|O60506|HNRPQ_HUMAN	Heterogeneous nuclear ribonucleoprotein Q	0.4601	0.4694	0.4722
9	sp|Q02818|NUCB1_HUMAN	Nucleobindin-1	0.4183	0.4681	0.4669
10	sp|P23142|FBLN1_HUMAN	Fibulin-1	0.3089	0.3163	0.5901
11	sp|P43490|NAMPT_HUMAN	Nicotinamidephosphoribosyltransferase	0.3585	0.39	0.3082
12	sp|P35527|K1C9_HUMAN	Keratin, type I cytoskeletal 9	0.198	0.2693	0.3428
13	sp|P21333|FLNA_HUMAN	Filamin-A	0.2026	0.2933	0.2692
14	sp|P49327|FAS_HUMAN	Fatty acid synthase	0.2589	0.2778	0.2049
15	sp|P02765|FETUA_HUMAN	Alpha-2-HS-glycoprotein	0.1842	0.2825	0.2596
16	sp|P06744|G6PI_HUMAN	Glucose-6-phosphate isomerase	0.2232	0.2356	0.2156
17	sp|P68871|HBB_HUMAN	Hemoglobin subunit beta	0.0323	0.3144	0.3065
18	sp|P01024|CO3_HUMAN	Complement C3	0.1593	0.1745	0.1923
19	sp|P08107|HSP71_HUMAN	Heat shock 70 kDa protein 1A/1B	0.1196	0.1398	0.1387
20	sp|P05121|PAI1_HUMAN	Plasminogen activator inhibitor 1	0.1239	0.1186	0.1547
21	sp|P07195|LDHB_HUMAN	L-lactate dehydrogenase B chain	0.0951	0.1569	0.1266
22	sp|P12956|XRCC6_HUMAN	X-ray repair cross-complementing protein 6	0.0954	0.1503	0.0884
23	sp|P02768|ALBU_HUMAN	Serum albumin	0.0698	0.1131	0.1014
24	sp|P01023|A2MG_HUMAN	Alpha-2-macroglobulin	0.0479	0.1067	0.1043
25	sp|P02788|TRFL_HUMAN	Lactotransferrin	0.065	0.103	0.0876
26	sp|P01033|TIMP1_HUMAN	Metalloproteinase inhibitor 1	0.0359	0.1211	0.0549
27	sp|P08670|VIME_HUMAN	Vimentin	0.0746	0.0708	0.0581
28	sp|Q92616|GCN1L_HUMAN	Translational activator GCN1	0.0461	0.0579	0.039
29	sp|P14174|MIF_HUMAN	Macrophage migration inhibitory factor	0.0365	0.0491	0.0344
30	sp|P01308|INS_HUMAN	Insulin	0.0184	0.025	0.0165
31	sp|Q96JB3|HIC2_HUMAN	Hypermethylated in cancer 2 protein	0.0118	0.0213	0.0011

Note: Only proteins in the CCA cell lines compared with H69 and have < 0.6-fold change were collected in this table. [a]Websites to access the data to the listed proteins: http://www.ncbi.nlm.nih.gov. [b]WD:N, [c]PD:N and [d]MD:N correspond to intensity ratio of OCA17:H69, K100:H69 and M156:H69, respectively. OCA17, well differentiated adenocarcinoma cell line; M156, moderately differentiated adenocarcinoma cell line; K100, poorly differentiated adenocarcinoma cell line; H69, non-malignant biliary cell line.

A. AnnexinA2 (sp|P07355|ANXA2_HUMAN)

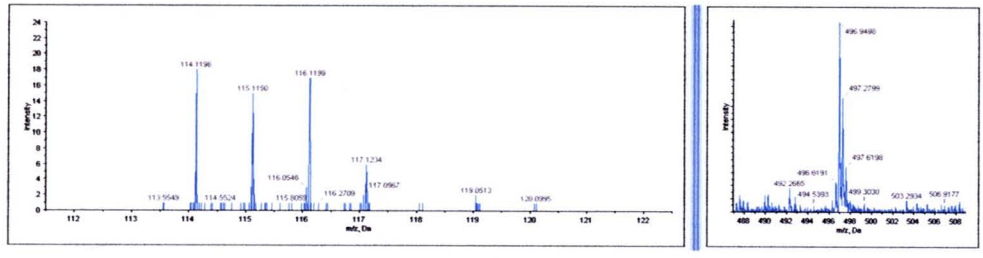

B. Transgilin-3 (sp|Q9UI15|TAGL3_HUMAN)

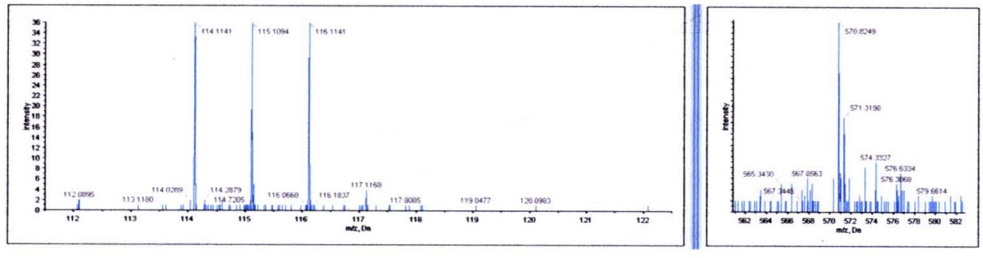

C. Insulin (sp|P01308|INS_HUMAN)

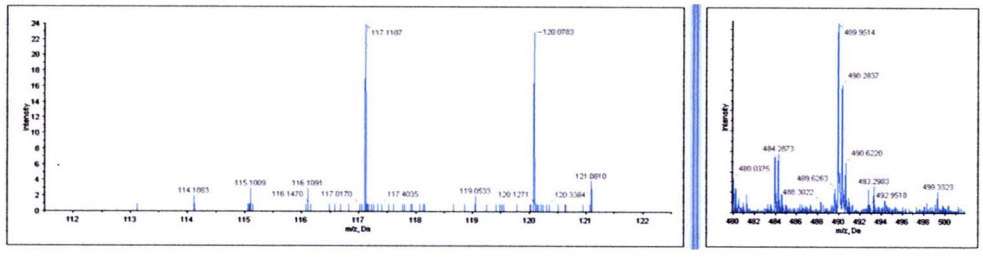

D. Macrophage inhibitory factor (sp|P14174|MIF_HUMAN)

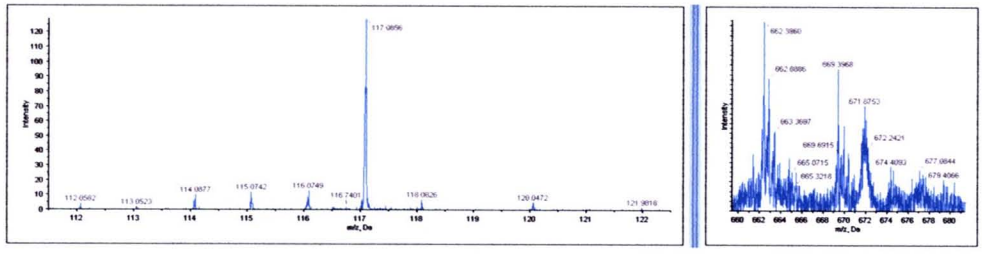

Figure 5.3 Peak areas at the low mass/charge *(m/z)* end showing a relative abundance of the up-regulated (A-B) and down-regulated (C-D) proteins as represented in left panel. Tandem MS spectra of (A) Annexin A2, (B) Transgelin-3, (C) Insulin and (D) Macrophage inhibitory factor represented in right panel. OCA17, M156, K100 and H69 cell lines were labeled with the 114, 115, 116 and 117 tags, respectively.

5.3.4 Validation of differential expression proteins

The differential expression levels of the proteins identified by iTRAQ approach were validated using immunohistochemistry analysis. In this study, three protiens including cathepsin-D (CATD), catenin delta-1 (CTND1) and transgelin 3 (TAGL3) were chosen for further analysis. As expected, mild expression of CATD was observed in the cytoplasm of normal bile duct epithelium and hepatocyte. In contrast, CATD was exclusively expressed in the cytoplasm of CCA tissues both papillary and tubular type. Additionally, significant up-regulated CATD was also observed in bile duct hyperplasia (Figure 5.4). Similar to CATD, the over-expression of CTND1 was detected in the cytoplasm of CCA both tubular and papillary type, while in bile duct hyperplasia CTND1 showed absent expression (Figure 5.5). In our IHC analysis, however, TGLN3 was observed to be absent in bile duct epithelium both under normal and in CCA conditions, while moderate expression was detected in positive control i.e., normal colon tissue (Figure 5.6).

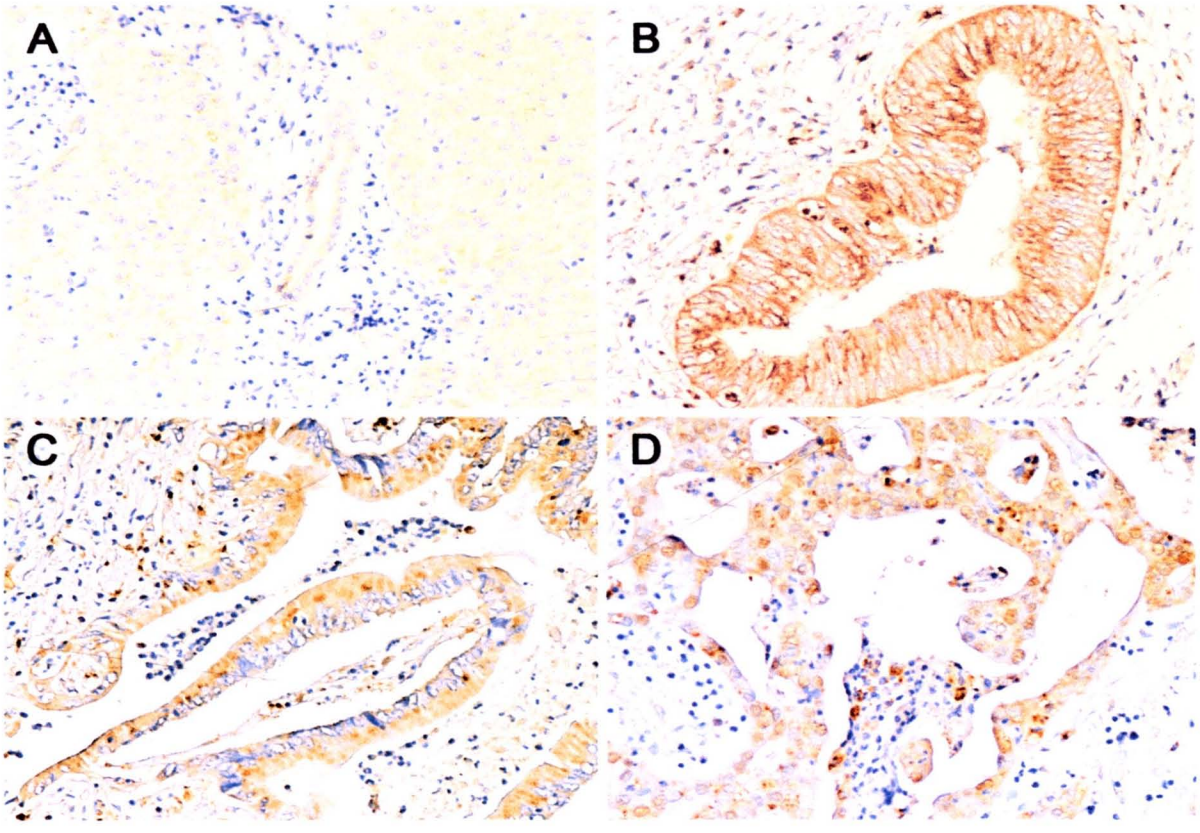

Figure 5.4 Tissue sections of cholangiocarcinoma-immunostained cathepsin D (CATD). Weak expression of CATD was shown in corresponding normal liver tissue (A), while strong expression of CATD was observed in the cytoplasm of bile duct hyperplasia (B) and CCA tissues both papillary (C) and tubular type (D). Original magnification x200 (A-D).

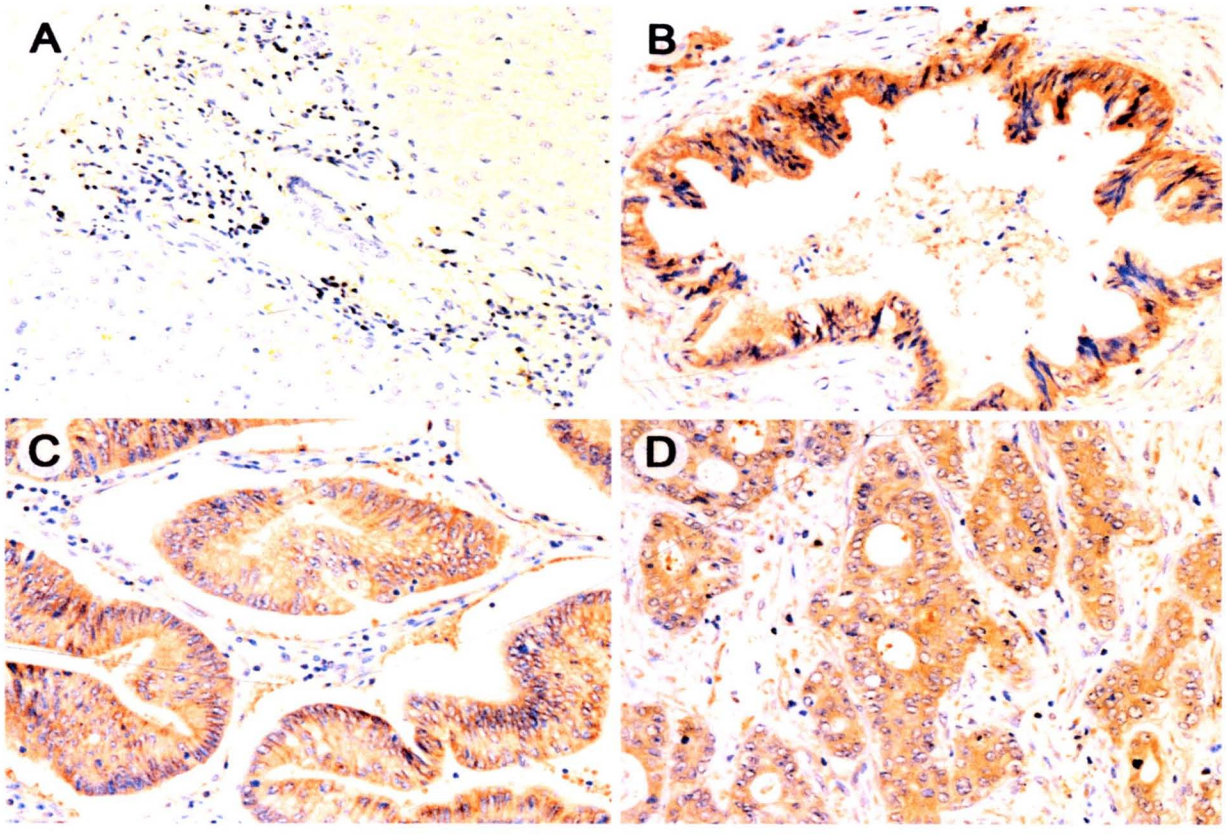

Figure 5.5 The expression of catenin delta 1 (CTND1) in CCA tissues detected by immunohistochemistry. (A) Very low expression of CTND1 was observed in the cytoplasm of normal liver tissue. In contrast, exclusively CTND1-expressed cells were clustered within bile duct hyperplasia and CCA tissues both papillary and tubular type. CTND1 was preferably cytoplasm in location of bile duct hyperplasia and CCA tissues. Original magnification x200 (A-D).

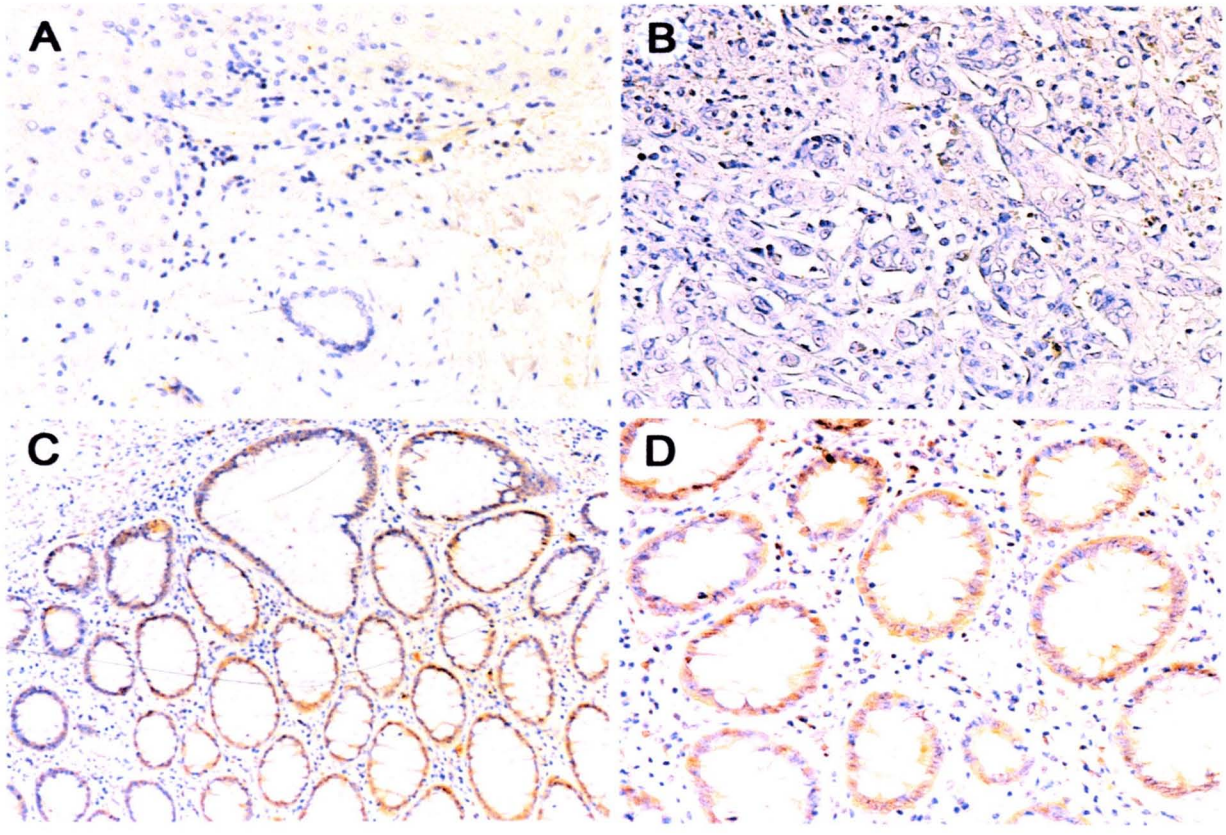

Figure 5.6 Immunoreactivity of transgelin 3 (TGNL3) in normal liver (A), bile duct cancer (B) and normal colon tissue (C-D). Original magnification: x100 (C), x200 (A-B and D). In our study, TGNL3 was observed to be absent in bile duct epithelial cells under normal and in cholangiocarcinoma (CCA) condition, while moderate staining was shown in positive control i.e., normal colon tissues.

Discussion

Here, an iTRAQ workflow was used to identify and quantify cholangiocarcinoma-associated proteins by comparing the whole cell lysate proteomes of three CCA cell lines including: K100, poorly differentiated adenocarcinoma; M156, moderately differentiated adenocarcinoma and OCA17, well differentiated adenocarcinoma with H69, a control normal biliary cell line. By utilizing the cutting edge proteomic techniques, we identified and quantified a total of 628 proteins including 232 differentially expressed proteins (201 up- and 31 down-regulated proteins). All identified 628 proteins were found to cover a wide range of subcellular localizations and biological processes. This illustrates the advantage of our approach in candidate biomarker identification with an improvement in proteome coverage.

With regard to false discovery rate (FDR) commonly used in quantitative proteomics, recent study reported that the advantage of the local FDR method over the global method was particularly obvious because the error rate of each protein was individually measured at the local FDR, while the global FDR only measures the error rate of the entire protein set (Wertz et al., 2008). This knowledge enabled us to decide which set of proteins to accept for further analysis while maintaining the error rate at a reasonable level. Thus, only proteins above the threshold were accepted for result interpretation. For example, in Table 5.4, thresholding at a local FDR of 1% would lead us to accept 628 proteins, but note that at the global FDR of our identification set (680 proteins) is 7.64% higher chance of being wrong for the interpretation. In this regard, the results suggest that thresholding based on the local FDR is the better approach because it assures that all reported identifications in our accepted set of proteins have at least some minimal quality. By contrast, if thresholding is based on a global FDR, the quality of the poorest identification in our set of proteins is unknown and not amenable to the interpretation.

Table 5.4 Number of protein identified at critical false discovery rates (FDRs)

Critical Value	Number of Proteins Detected[a]		
Accepted FDR	Local FDR	Global FDR	Global FDR from Fit
1.00%	628	680	678
5.00%	644	768	760
10.00%	652	863	

Note:[a]The protein identification scores outputted by database search algorithm were weighted by their discriminating power using a Shannon information entropy based strategy (Wang et al., 2009).

Among the differentially expressed proteins, several up-regulated proteins have been reported in other proteomic studies such as heterogeneous nuclear ribonucleoproteins K (hnRNP K) (Wen et al., 2010), utrophin (Chang et al., 2007), caein kinase II (Jia et al., 2010), lamin-B1 (Sun et al., 2010), transgelin 3 (Lee et al., 2010), delta-catenin (Zeng et al., 2009) and cathepsin-D (Merseburger et al., 2005). Additionally, iTRAQ analysis could identify annexin A2 (ANXA2) to be over-expressed in all CCA cell lines compared to a control H69, confirming our previously published data (Yonglitthipagon et al., 2010). Furthermore, the under-expression of calreticulin in our study has been proposed as an early event in tumor carcinogenesis of many cancers (Alur et al., 2009) and may contribute to tumor suppressor in CCA.

In addition, a large number of up-regulated differentially expressed proteins in CCA cell lines were related to signal transduction. 14-3-3 protein is a ubiquitous family of biomolecules that participate in positive regulation of the MAPK and the PI3K/AKT pathways which are associated with the ability of cancer cells to proliferate in an uncontrolled manner (Tzivion *et al.*, 2006). Elevated expression of 14-3-3 protein (theta isoform) was observed in our study, suggesting that 14-3-3 protein may have important roles in CCA carcinogenesis. Another finding was that the ion transporters such as chloride intracellular channel protein 1 (CLIC1), voltage-dependent anion-selective channel proteins 1,2 and 3 (VDAC1-3) were all up-regulated in CCA cell lines. It was reported that over-expression of CLIC1 could modulate cell division and apoptosis, resulted in enhancing tumor transformation (Huang *et al.*, 2004). VDACs which are essential for mitochondrial-dependent apoptosis were found to express at higher levels in cancer cells (Simamura *et al.*,

2006). The findings herein suggest that dysregulation of these ion transporters may play important roles during carcinogenesis of CCA.

Likewise, many up-regulated oxidoreductases including peroxiredoxin 1, peroxiredoxin 4, isocitrate dehydrogenase (subunit gamma) and thioredoxin reductase have been reported that were closely correlated with the development of multidrug resistant by other research effort (Naito et al., 1999). Moreover, cell migration is a cyclical process that is largely driven by the polymerization and depolymerization of the actin cytoskeleton by a tightly regulated process that integrates cellular signals to drive reorganization of actin microfilaments in a concerted manner (Olson et al., 2009). As might be expected, over-expressed actinin-1 in this study has been previously reported that the interaction between actin microfilaments with the cell membrane and, indirectly, to collagen 12 alpha 1 in the extracellular matrix resulting in tumor invasion were mediated by the over-expression of actinin-1 (Gonzalez *et al.*, 2001).

Of particular interest, three proteins including cathepsin-D (CATD), catenin delta-1 (CTND1) and transgelin 3 (TGLN3) proteins in which have not been studied previously in CCA, were subsequently verified using immunohistochemistry (IHC). Firstly, cathepsin-D was identified as a 52-kDa estrogen-regulated secretory glycoprotein with autocrine mitogenic activity in breast cancer (Westley et al., 1980). Many biological roles have been attributed to CATD, including (Westley et al., 1996): degradation of the extracellular matrix, increasing cells' malignant phenotype and metastatic potential, stimulation of (metastatic) cell proliferation by increasing the local bioavailability of growth-stimulatory growth factors, inactivation of a growth inhibitor and prevention of apoptosis. Secondly, although abnormal expression of p120ctn (CTND1's homologue) was found to associate with poor prognosis of cancers; however, little is known about the significance of the expression status of CTND1. It was reported that CTND1 could bind to the juxtamembrane domain (JMD) of E-cadherin and the zinc finger domain of Kaiso (a transcriptional repressor) in cytosol of tumor cells to enhance the invasive ability of tumor cells by regulating the activity of small GTPases. Additionally, its over-expression could also change the cell cycle from the G1 stage to the S and G2/M stage resulting in significantly increased the proliferation ability of tumor cells (Lu et al., 1999; Rodova et al., 2004). In

addition, the over-expression of CTND1 was significantly associated with poor prognosis in non-small cell lung cancer (Zhang et al., 2010) and prostate cancer patients (Lu et al., 2005). However, the clinical significance of CTND1 have not been defined in CCA until now. Using IHC analysis, the over-expression trends of CATD and CTND1 in human CCA tissues compared to control normal liver tissues were similar to the protein expression levels obtained in iTRAQ approach. The consistent over-expression of CATD and CTND1 were observed in both papillary and tubular types of human CCA. As a precancerous disease, bile duct hyperplasia also exhibited high expression levels of CATD and CTND1 in contrast to the relative absence of their expression in normal hepatocytes and cholangiocytes, suggesting that CATD and CTND1 may contribute to the cholangiocarcinogenesis. These findings indicate that CATD and CTND1 may represent novel biomarkers for predicting progression and prognosis of CCA. Therefore, the significant association of CATD and CTND1 levels with CCA clearly requires further investigation. Finally, transgelin 2 (TGLN2) and transgelin 3 (TGLN3) were significantly up-regulated in CCA cell lines and represent potential biomarkers that have not been identified previously. TGLNs have been shown to bind and colocalize with F-actin, indicating that TGLNs may be involved in cell differentiation by stabilizing the cytoskeleton through actin binding (Marchler-Bauer *et al.*, 2007). Furthermore, diminished expression of these proteins have been reported in a variety of cell types on transformation as well as in several human cancers such as colon cancer (Friedman *et al.*, 2004), esophageal squamous cell carcinoma (Qi *et al.*, 2005) and gastric cancer (Huang *et al.*, 2008). Within the protein expression levels obtained in iTRAQ analysis, TGLN3 exhibited higher expression in CCA cell lines compared to TGLN2 (21.13- and 1.83-fold, respectively). In this regard, studies have pointed out that TGLN2 and TGLN3 may also contribute the CCA carcinogenesis. Regarding its expression level obtained in iTRAQ approach, TGLN3 was selected for further verification in human CCA tissues. However, as a marker filtered from cell lines *in vitro*, its clinical significance is sometime limited (Hay et al., 1988). In our study, the expression of TGLN3 was not detected by using IHC in human CCA as well as normal corresponding liver tissue (both hepatocyte and cholangiocyte). In contrast to moderate-strong expression of TGLN3 was clearly visualized in a positive control i.e., normal colon tissue. Although, the IHC could not

confirm the direction of TGLN3's change observed in iTRAQ approach, other studies, however, has already reported this discrepancy (Keshamouni et al., 2006).

In conclusion, the strategy combining iTRAQ analysis and LC-MS/MS was used to profile proteomic changes in CCA cell lines compared to a control H69 cell line. Many previously reported potential tumor markers could be identified, supporting the strategy employed in this study. More importantly, this study identified a number of novel differentially expressed proteins in CCA cell lines compared to H69. In particular, the expression levels of the protein CATD and CTND1 differed significantly between the normal and CCA tissues, suggesting that they may contribute to the CCA carcinogenesis and also serve as novel biomarkers for predicting tumor progression and prognosis. Therefore, the assessment of CATD and CTND1 protein expressions in conjunction with CCA is clearly required for further investigation.